ISSN 8756-6990, Optoelectronics, Instrumentation and Data Processing, 2018, Vol. 54, No. 1, pp. 1–8. © Allerton Press, Inc., 2018.
Original Russian Text © D.D. Ruzhitskaya, A.A. Samoilenko, A.D. Ivanov, K.N. Min'kov, 2018, published in Avtometriya, 2018, Vol. 54, No. 1, pp. 71–79.

OPTICAL INFORMATION TECHNOLOGIES

Analysis of the Transmission Spectra of Optical Microcavities Using the Mode Broadening Method

D. D. Ruzhitskaya[a,b], A. A. Samoilenko[b], A. D. Ivanov[b], and K. N. Min'kov[b,c]

[a] *Lomonosov Moscow State University, Leninskie Gory 1, Moscow, 119991 Russia*
[b] *All-Russian Scientific Research Institute of Optical and Physical Measurements, ul. Ozernaya 46, Moscow, 119361 Russia*
[c] *Tikhonov Moscow Institute of Electronics and Mathematics, National Research University of Higher School of Economics, ul. Myasnitskaya 20, Moscow, 101000 Russia*
E-mail: Academi@ya.ru

Received August 2, 2017

Abstract—This paper presents an algorithm for processing the transmission spectra of whispering-gallery optical microcavities for use as a nanoparticle detector. The algorithm is based on the broadening of the microcavity resonance curve during precipitation of nanoparticles on the microcavity surface. Experimental results on the detection of particles are compared with Langmuir adsorption theory. The contribution of the instability of the excitation radiation source due to the temperature drift of the resonant frequency to the measurement error is estimated.

Keywords: optical microcavities, optical sensor, nanoparticles, whispering-gallery modes, Langmuir adsorption theory.

DOI: ?

INTRODUCTION

Optical dielectric microcavities (ODMC) are bodies of revolution made of optically transparent material. On the inner surface of the ODMC, near its equator, radiation can propagate on a closed trajectory and the formation of optical resonances is possible. Such resonant modes are called whispering-gallery modes. They have high quality factors and can therefore be used to determine small fluctuations in the refractive index in the environment with high sensitivity [1]. The high sensitivity of the transmission spectra of ODMC to various inhomogeneities makes it possible to use them as sensors for detecting nanosized particles [2].

The principle of the developed adsorption sensor is based on the following phenomenon. Nanoparticles that settle on the ODMC surface near its equator are related to the whispering-gallery mode emission through the dropping field. As a result of this interaction, part of the cavity mode emission scatters in the environment, and part of the emission returns back to the cavity. Backscattering leads to degeneracy of the initial mode and the formation of two new modes (propagating clockwise and counterclockwise), and the scattering in the environment to optical-resonance losses, which, in linear oscillatory systems, contribute to the broadening of the resonance curve [3]. Thus, the adsorbed particles cause a broadening of the transmittance spectrum of the ODMC. Spherical particles of the same diameter attached to the ODMC surface will lead to different losses depending on the location of the particle relative to the spatial localization of the field [4]. However, for a large number of such particles, this effect will be averaged, and in this case, we can assume that the losses are proportional to the number of nanoparticles deposited on the ODMC.In general, the mode broadening method provides information on single particles, and this has been confirmed

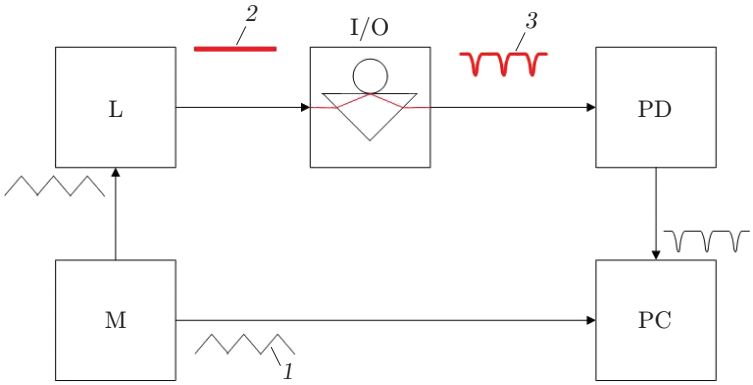

Fig. 1. Block diagram of the signal detection system ((*1*) clock signal, (*2*) optical emission, (*3*) ODMC transmission spectrum).

by experiments [5]. In the present study, the diagnostic parameter was the width of the optical-mode resonance curve, which is proportional to the energy losses in the mode and, consequently, to the number of adsorbed particles. The concentration of nanoparticles in the sample is determined from the rate of their deposition on the ODMC surface.

Thus, to develop a measuring system using a ODMC as a primary converter, it is necessary to process its transmission spectrum in order to determine the width of the whispering-gallery mode resonance curve at each measurement time.

EXPERIMENTAL SETUP

To measure the concentration of nanoparticles, we developed a detection system whose block diagram is shown in Fig. 1. A tunable laser (L) with a Vita Wave ECDL-6710R external cavity was used; due to this, the wide spectral line of the diode laser is converted into a narrow one [6]. The signal is obtained as follows. The frequency modulator (M) included in the laser control unit generates a signal that affects the laser frequency tuning system. This signal has a sawtooth shape and contains regions of rise (forward pass) and fall (reverse pass). The signal is then fed to the laser frequency tuning channel and is recorded by a personal computer (PC) using an ADC (clock signal). Radiation input and output in the ODMC is carried out using an input/output (I/O) system, which is a triangular prism. The laser beam focuses on the inner surface of the prism at a larger angle than the total internal reflection angle. If the ODMC is brought to a distance of the order of the wavelength from the focal point, the total internal reflection begins to be violated and some of the light from the prism enters the ODMC and back into the prism. This provides coupling with the ODMC. If the whispering-gallery scanning mode of the ODMC falls in the laser frequency scanning range, the radiation power transmitted through the I/O system begins to be absorbed by the mode. In this case, a negative peak appears in the photodetector (PD) signal at a corresponding frequency which characterizes the ODMC radiation absorption during nanoparticle adsorption on the ODMC surface. The resulting transmission spectrum of the microcavity and the clock signal from the laser control unit is recorded using the ADC for further processing.

PROBLEM STATEMENT

It is necessary to develop an algorithm for processing the ODMC transmission spectrum which will allow calculation of the concentration of nanoparticles in air or liquid media during their interaction with the ODMC surface.

DETERMINING THE TIME DEPENDENCE OF THE CHANGE IN THE WIDTH OF THE RESONANCE CURVE

Data processing and finding the concentration of nanoparticles are carried out using MATLAB software. The signal is used to perform three sequential operations: selection of successive transmission spectra of the ODMC from the record for a fixed laser frequency scanning range, normalization and alignment of the

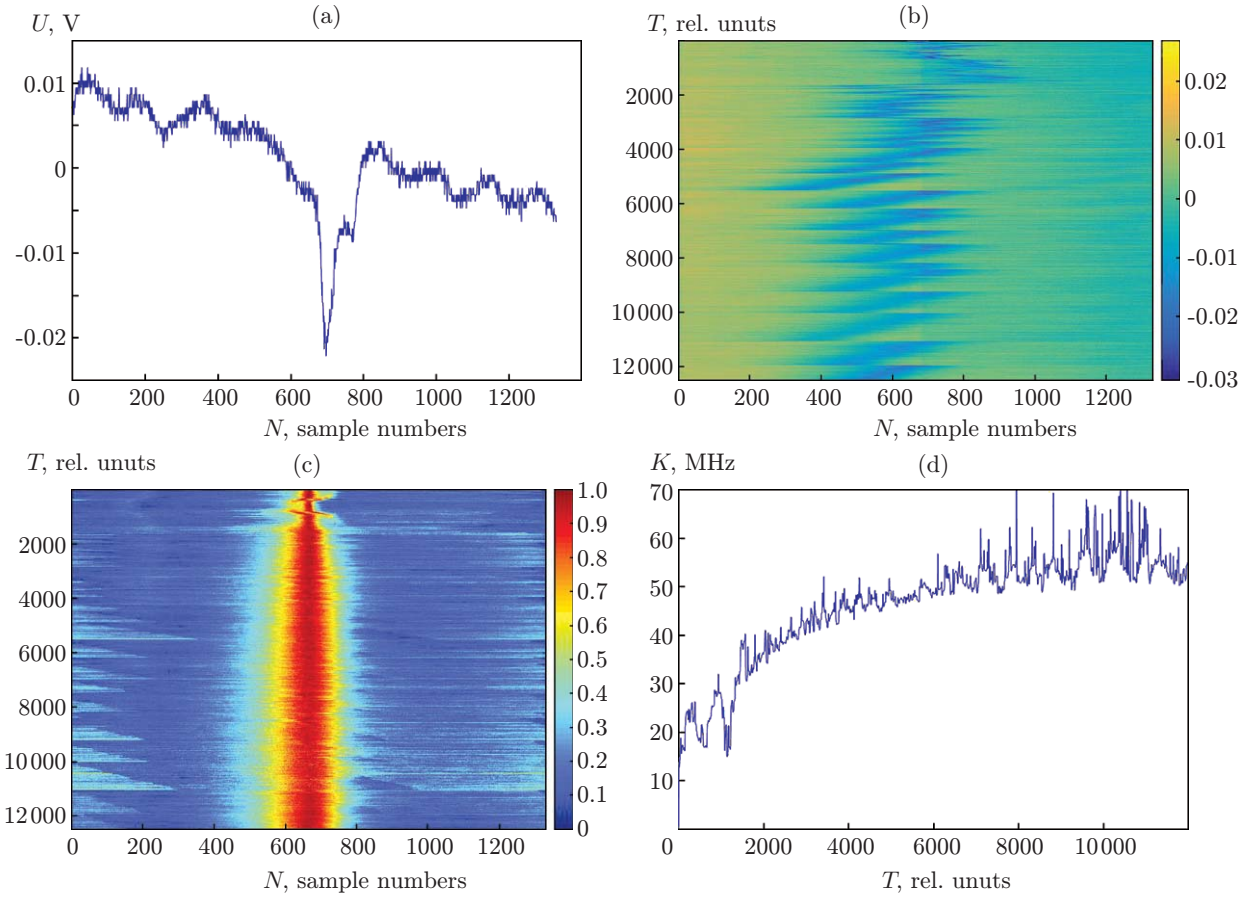

Fig. 2. Sequence of signal processing: (a) single realization of change in the transmission spectrum of the ODMC; (b) frequency spectrum of the ODMC; (c) aligned frequency spectrum of the ODMC normalized to 1 without drift; (d) width of the resonance curve after filtering.

sequence of transmission spectra of microcavities, and calculation of the time dependence of the width of the resonance curve.

The first stage of processing of ODMC transmission and clock signals involves their division into two components: the forward and reverse passes of laser frequency scanning. For this, the period of the clock signal T is determined by its Fourier spectrum [7]. Next, the clock signal is partitioned into the regions of forward and reverse passes:

1) the search interval is specified in the form$[A_0, A_0 + T]$, where A_0 is the initial search point, the period T is determined by the maximum in the clock signal spectrum obtained by means of a discrete Fourier transform;

2) a local maximum is found in the selected region;

3) the end of the clock signal is verified, a new value of A_0 is specified, and transition to the next interval occurs.

Further, the entire transmission spectrum of the ODMC is cut into single realizations of the spectra in such a way that the same sample numbers in each realization correspond to the same laser frequency. This operation is performed as follows. The beginning of a single transmission spectrum of the ODMC is assumed to be the position of the maximum obtained in Subsection 2, and its length is $T/2$. A single realization of the ODMC transmission spectrum is given in Fig. 2a, where U is the ADC signal level and N are the sample numbers. After this, a matrix is compiled in which each row represents a single realization of the spectrum. The thus obtained set of realizations makes it possible to analyze the cavity mode at the same laser frequency.

An image of the matrix is shown in Fig. 2b. The spectrum frequency is 25 Hz (set by the laser control unit). Color denotes the signal intensity from 0 to 1 in normalized units.

At this stage, there is a drift in the resonance frequency of the ODMC transmission spectrum associated with a temperature change and the corresponding deformation of the cavity. The broken form of the transmission spectrum is also due to the fact that, during the measurement, the operator corrected the center frequency of laser tuning in such a way that the resonance peak did not leave the scanning region of the detection system.

The second stage of processing is the normalization and alignment of the matrix of single transmission spectra of the microcavity. This stage involves three steps:

1. The linear slope caused by the change in the power due to laser frequency tuning and manifested in the slope of the constant component of the optical radiation is subtracted from each single realization of the ODMC transmission spectrum. The slope for each single realization is calculated from the values of the first and last points.

2. Each row is normalized to 1. For this, the maximum and minimum values of each single realization are calculated. The normalization is performed according to the formula

$$\mathrm{Norm}(j) = (\max_j - x(i)_j)/(\max_j - \min_j), \tag{1}$$

where Norm is the value of the normalized aligned spectrum; j is the spectrum realization number; $x(i)$ is the value of the i-th point in the j-th single realization of the spectrum; $\max_j$ and $\min_j$ are the maximum and minimum values in this realization.

3. Alignment of the resonance maximum. This operation is performed using the following algorithm:

a) a mask matrix is composed of 0 and 1 (position 1 corresponds to the presence of a peak in this region, and position 0 to its absence), which is calculated by the formula

$$\mathrm{Mask} = \mathrm{sign}(\mathrm{Norm} - \mathrm{Thr})/2 + 0{,}5, \tag{2}$$

where Thr is the threshold value for the peak search, which varies from 0 to 1 (for the given realization of the spectrum, it is set equal to 0.85); sign(Norm − Thr) is a function defined as

$$\mathrm{sign} = \begin{cases} 1, & \mathrm{Norm} - \mathrm{Thr} \geq 0, \\ -1, & \mathrm{Norm} - \mathrm{Thr} < 0; \end{cases}$$

b) a function is composed which displays the position of the coordinate of the center of the peak x_c^j in each j-th row and has the form

$$x_c^j = \sum_i x_i m_i^j \Big/ \sum_i m_i^j, \tag{3}$$

where x_i is the current coordinate of the point in the j-th single realization of the spectrum and m_i^j is the value of the i-th sample of the j-th single spectrum;

c) in each single realization of the spectrum, the peak is shifted to the central position using the built-in MATLAB cyclic permutation function.

The normalized transmission spectrum of the ODMC from which the drift component is subtracted is shown in Fig. 2c. The aligned frequency spectrum obtained in this way gives an idea of how the broadening of the resonance curve occurred, and makes it possible to determine the presence of interruptions in the operation of the sensor.

The third stage involves the generation of a mask of the aligned frequency spectrum in the form of combinations of 0 and 1 by formula (2). The threshold Thr is chosen equal to 0.5, which corresponds to half the height of the peak. Summation of the rows of this matrix yields a curve that describes the dependence of the width of the peak on time (Fig. 2d). The sample values are converted to the values of the optical frequency K using the laser scanning amplitude, which is determined by the signal from a reference interferometer using the scale factor

$$k = T_{\mathrm{MHz}}/T_{on}, \tag{4}$$

where T_{MHz} is the laser frequency scanning amplitude determined by the reference interferometer (T_{MHz} is set by the operator); T_{on} is the length of the single spectrum in the samples. The signal of the reference interferometer and clock and transmission signals are recorded simultaneously.

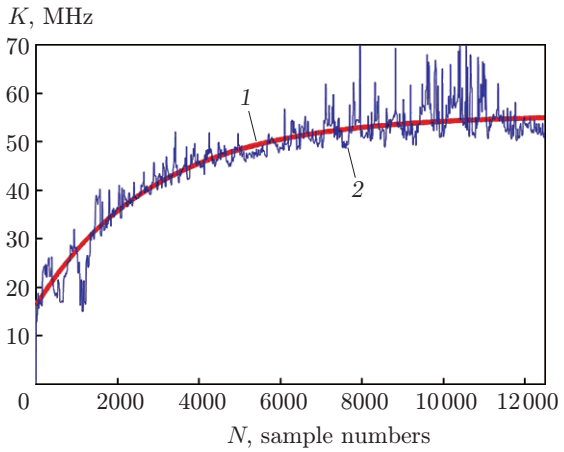

Fig. 3. Comparison of the theoretical curve (*1*) characterizing the coverage of the ODMC with particles and the experimental curve of mode broadening (*2*).

The recalculated curve is subjected to linear filtering with zero phase. An advantage of this filter is that it preserves the signal shape in its time domain [8]. Thus, the influence of random fluctuations in the laser frequency, the noise of the radiation receiver, and local surges due to vibration can be minimized.

INTERPRETATION OF THE DATA OBTAINED

The curve in Fig. 2d has a region of linear growth. The slope of this region is proportional to the deposition rate of nanoparticles on the ODMC surface. To find the particle concentration in the medium, calibration is carried out using a reference sample, and the proportionality coefficient between the rate of broadening of the resonance curve and the nanoparticle concentration in the medium.

It should be noted that during particle deposition, not every collision ends with particle adhesion to the ODMC surface. The probability of this event is proportional to the particle concentration and depends on the surface properties of the microcavity and the degree of coverage of the surface with the particles deposited earlier. Thus, at the initial time when the surface of the microcavity is "clean" and the number of adhesion centers to which particles can adhere is much larger than the number of the already deposited particles, and the number of particles deposited per unit time is constant. Furthermore, the number of particles on the surface and, consequently, the width of the resonance curve of the optical mode also increase linearly. When the amount of deposited particles becomes large so that they began to prevent the adhesion of new particles, the rate of their deposition decreases and then goes to saturation. This phenomenon is represented by the adsorption theory with the formation of a layer of particles. The obtained result agrees with Langmuir adsorption theory [9]. The model of particle adsorption on the microcavity surface is described by the equation

$$\frac{d\theta}{dt} = k_\alpha C_0(1-\theta) - k_d\theta, \tag{5}$$

where k_α and k_d are the adsorption and desorption constants; C_0 is the concentration of adsorbing particles; θ is the degree of coverage of the microcavity surface.

The theoretical calculation of the deposition of nanoparticles on the ODMC surface is shown by curve *1* in Fig. 3. As can be seen from the figure, the solution of Eq. (5) well approximates the experimental curve of mode broadening (*2*).

DETERMINATION OF THE INFLUENCE OF THE FREQUENCY INSTABILITY OF THE LASER ON THE WIDTH OF THE RESONANCE PEAK

It can be seen from Fig. 2b that in the ODMC spectrum during the measurements, there is a drift of the resonant frequency with the corresponding laser frequency tuning. The tunable laser is the source of

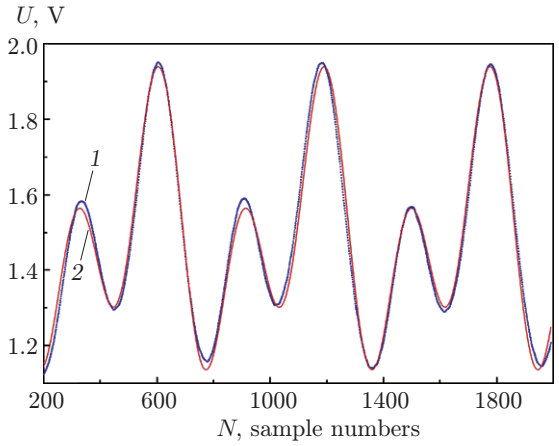

Fig. 4. Comparison of the signal from the reference interferometer (curve *1*) with the model $S_{\text{mod}}(x)$ (curve *2*) to estimate the relative distortions.

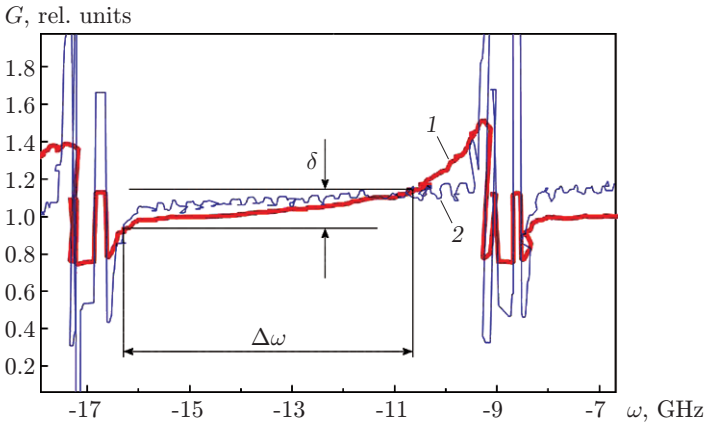

Fig. 5. Fluctuations in the amplitude of the frequency swing (curve *1*) and the mode shape parameter (curve *2*) depending on the center frequency of the laser ω.

frequency instability due to the competition of modes and sharp changes in the build-up amplitude during mode hopping and introduces an error into the result of measuring the width of the resonance curve. In determining the optimum laser operation conditions, we evaluated the contribution of the center lasing frequency to the instability of the frequency swing amplitude. To solve this problem, the signal recorded from the reference interferometer with a gradual change in the center frequency of the laser was analyzed. The laser beam was directed to the ring interferometer, and the signal was taken from the photodetector. When recording the signal, the operator slowly varies the center frequency, resulting in a sequence of interferograms in the form of frames (Fig. 4). This signal is well described by the sum of two sinusoids. To estimate the distortions of the interferogram during the tuning of the center frequency of the laser, we constructed the signal model

$$S_{\text{mod}}(x) = P + A\sin(\omega(x - x_0)) + K_1 A\sin(2\omega(x - x_0) + \Delta\varphi), \tag{6}$$

where P is the constant component of the signal; A is the amplitude of the first harmonic; K_1 is the coefficient of proportionality between the first and second harmonics; $\omega = 2\pi/T$ is the center frequency of the laser; $\Delta\varphi$ is the phase; x_0 is a parameter that characterizes the displacement of the constant frequency component.

The laser tuning characteristics were analyzed using the following algorithm. The record of the signal from the reference interferometer was divided into single realizations using a clock signal according to the

algorithm described above. The total number of frames for the analysis was 1400. For each frame, fitting with the model (6) was successively carried out. The results of processing the interferogram frames are shown in Fig. 5. Here curve *1* characterizes the parameter T responsible for the amplitude of the frequency swing, and the parameter K_1 (curve *2*) for distortion of the waveform reflecting the processes in the laser.

The full range of center frequency tuning is about 15 GHz. In the region with local ouliers of the parameter K_1, transient processes are observed in the laser cavity, so that the correct calculation of the parameter T in this region is impossible. In addition, near the regions, the steepness of the parameter T increases; therefore, it is not recommended to use this frequency region in the presence of temperature drift of the resonant frequency of the ODMC. Nevertheless, in the full range of the transient behavior includes a region of width $\Delta\omega \approx 5$ GHz with a gentle slope, where the change in the swing amplitude δ does not exceed 25%. This region provides an acceptable error for a wavelength shift in range 1 GHz due to the adsorption of nanoparticles and the influence of temperature.

CONCLUSIONS

An algorithm for processing the spectra of ODMC to obtain quantitative estimates of the concentration of nanoparticles adsorbed on its surface was described. This algorithm allows the calculation of resonance peak broadening under conditions of temperature drift of the frequency and was used to study the deposition of silver nanoparticle in a liquid medium [10] and TiO_2 nanoparticles in air. In real-time experiments, fluctuations in the width of the resonance peak were observed, which could correspond to acts of interaction (adsorption or collision) of single particles with the ODMC surface. In the experimental tests of this method, the minimum recorded mass concentration of nanoparticles was 0.001 ppm and the maximum value was 1 ppm. Theoretically, the upper concentration limit in the employed algorithm will be limited by the laser scanning speed. Analysis of the curves obtained by processing spectra using the proposed algorithm indicates the formation of a monolayer of particles on the ODMC surface. The standard deviation of concentrations in the experiments was about 15%. This result is consistent with adsorption theory, and the broadening of the mode can be approximated by the Langmuir isotherm. The accuracy of approximation was estimated by a determination coefficient $R_{\text{sqr}} = 0.789$. The value of the coefficient indicates that the approximation is good enough. The particle shape and size can affect the deposition rate and the dynamics of displacement in the medium under study, and the polarizability of particles can influence the loss of absorption [3], but to a greater extent, the shift of the resonant frequency [2]. For this reason, it is necessary to calibrate the sensor taking into account the average diameter and type of the nanoparticles under study. For detection purposes, one should use a ODMC with a quality factor of not less than 10^6, which appreciably depends on the surface roughness.Roughness control before the use of ODMC can be carried out by interference microscopy [11]. In addition, a modification of the algorithm was developed to determine the laser frequency tuning characteristics and to estimate instability. The instability of the optical pump source was found to have no significant effect on the calculation of the nanoparticle concentration in the investigated medium provided that the laser operates in a given frequency range. Despite the fact that the algorithm includes compensation of the resonance shift, to reduce the error and improve the results, it is important to provide thermal stabilization of the measuring cell and the medium studied.

The work was performed using the equipment of the Center for collective use of high-precision measuring technologies in the field of photonics [12], established on the basis of the All-Russian Research Institute of Optical and Physical Measurements.

We are grateful for useful discussions to Professor G. G. Levin, Head of the Department of Holography, Optical Tomography, Nanotechnology, and Nanomaterials of the All-Russian Research Institute of Optical-Physical Measurements.

REFERENCES

1. M. L. Gorodetskii, *Optical Microcavities with Giant Q-Factor*, (Fizmatlit, Moscow, 2011) [in Russian].
2. M. R. Foreman, J. D. Swaim, and F. Vollmer, "Whispering Gallery Mode Sensors," Adv. Opt. and Photon. **7** (2), 168–240 (2015).
3. Y. Hu, L. Shao, S. Arnold, et al., "Mode Broadening Induced by Nanoparticles in an Optical Whispering-Gallery Microcavity," Phys. Rev. **90** (4), 043847 (2014).
4. J. Wiersig, "Structure of Whispering-Gallery Modes in Optical Microdisks Perturbed by Nanoparticles," Phys. Rev. A **84** (6), 063828 (2011).

5. L. Shao, X.-F. Jiang, X.-C. Yu, et al., "Detection of Single Nanoparticles and Lentiviruses using Microcavity Resonance Broadening," Adv. Mater. **25** (1), 5616–5620 (2013).
6. V. V. Vassiliev, S. A. Zibrov, and V. L. Velichansky, "Compact Extended-Cavity Diode Laser for Atomic Spectroscopy and Metrology," Rev. Sci. Instrum. **77** (1), 013102 (2006).
7. Ch. Van Loan, *Computational Frameworks for the Fast Fourier Transform*, (Philadelphia: SIAM, 1992).
8. J. O. Smith III, *Introduction to Digital Filters with Audio Applications*, (W3K Publishing, 2007).
9. P. Schaaf and J. Talbot, "Surface Exclusion Effects in Adsorption Processes," Journ. Chem. Phys. **91** (7), 4401–4409 (1989).
10. A. A. Samoilenko, G. G. Levin, V. L. Lyaskovsky, et al., "Application of Whispering-Gallery-Mode Optical Microcavities for Detection of Silver Nanoparticles in an Aqueous Medium," Optika and Spektroskopiya **122** (6), 1037–1039 (2017) [Optics and Spectroscopy **122** (6), 1002–1004 (2017)].
11. G. N. Vishnyakov, G. G. Levin, and V. L. Minaev, "Automated Interference Tools of the All-Russian Research Institute for Optical and Physical Measurements," Avtometriya **53** (5), 131–138 (2017) [Optoelektron., Instrum. Data Process. **53** (5), 530–536 (2017)].
12. *Center for Collective Use of High-Precision Measurement Technologies in the Field of Photonics*. URL: http://www.ckp.vniiofi.ru/ (access date: 2.08.2017).